Available online at www.sciencedirect.com
ScienceDirect
Journal of the European Ceramic Society 29 (2009) 1925–1932
www.elsevier.com/locate/jeurceramsoc

Densification additives for hydroxyapatite ceramics

T.V. Safronova [a,*], V.I. Putlyaev [a], M.A. Shekhirev [b], Y.D. Tretyakov [b], A.V. Kuznetsov [c], A.V. Belyakov [d]

[a] *Department of Chemistry, MSU, Vorobievi Gory, 1, Moscow 119991, Russia*
[b] *Materials Science Department, MSU, Vorobievi Gory, 1, Moscow 119991, Russia*
[c] *I.M. Sechenov Moscow Medical Academy, Trubetskaya street, 8 - 2, Moscow 119992, Russia*
[d] *Department of Chemical Technology of Silicates, MUCTR, Miusskaja pl., 9, Moscow 125047, Russia*

Received 17 May 2008; received in revised form 15 November 2008; accepted 9 December 2008

Abstract

The present work is aimed at the elucidation of the role played by $CaCl_2$ and NH_4NO_3 (the latter is a by-product of the solution synthesis of hydroxyapatite, hereinafter referred to as HAp) in the densification of nano-sized HAp powder in the course of the pressureless sintering. Nanocrystalline HAp powder was fabricated via the wet-precipitation technique by the dropwise addition of an $(NH_4)_2HPO_4$ solution to a $Ca(NO_3)_2$ mother solution at a pre-adjusted pH at 60 °C. The pH of the aqueous mixture was maintained at a constant value (either 7 or 9) by the addition of an appropriate amount of NH_4OH. The Ca/P ratio was set to 1.67, 1.61, and 1.48; 10 wt% of $CaCl_2$ was added to dry HAp powder. NH_4NO_3 remaining in unwashed HAp powder can act as a fluxing agent that promotes partial melting at a relatively low temperature (150–250 °C) thus allowing the particles to rearrange into a denser packing. Several mechanisms of the $CaCl_2$ action as a densification additive might be envisaged: (i) a decrease in the melting temperature; (ii) the surface wetting of grains; (iii) a change in the growth morphology owing to the high-temperature surfactant properties; (iv) a possible reaction with HAp on the surface of grains giving rise to the decomposition of HAp and yielding chlorapatite (ClAp), which can convert back to HAp over a wide temperature range and at any level of H_2O.

Keywords: Sintering; Powders-solid state reaction; Grain size; Apatite; Biomedical applications; Peritectic melting

1. Introduction

Ceramics based on calcium phosphates is widely recognized as a highly promising material for the human tissue restoration due to its excellent biocompatibility. Numerous works have been devoted to the conventional pressureless sintering of HAp ceramics in the solid-state regime under surface or volume diffusion control.[1–7] Another direction in the fabrication of HAp ceramics is based on the utilization of the liquid-phase sintering. There are two ways to improve on the densification of powder compacts in the course of the liquid-phase sintering. One of them consists in the addition of a fine glass powder, which is inert with respect to the main component(s). Another way consists in the addition of a powder, which can interact with the main crystalline phase of the compact after melting yielding a multi-component melt, presumably, an eutectic liquid. Typically, the liquid-phase sintering proceeds faster than the solid-state one.[8–12]

Various types of additives specific to HAp sintering have been considered by Suchanek et al.[13] They included different salts, *e.g.*, $CaCl_2$, KCl, KH_2PO_4, $(KPO_3)_n$, $Na_2Si_2O_5$, K_2CO_3, Na_2CO_3, KF, sodium phosphates; compounds within bi- and three-component oxide systems, including P_2O_5 and CaO. These additives were added to HAp powders in an amount of 5%. Takami and Kondo[14] described sintering and reinforcing additives (in the form of a frit) in the system P_2O_5–CaO near the eutectic composition (Ca/P = 0.2–0.7) in an amount of 5%. The phase formation in ceramics based on HAp and frit in the system P_2O_5–CaO in amount of 10–40% was also described.[15] Georgiou and Knowless[16] used additives from the ternary Na_2O–P_2O_5–CaO system. Tancred et al.[17] used glasses from the CaO–P_2O_5 system (with a CaO to P_2O_5 molar ratio of 1) in quantities of 2.5, 5, 10, 25, and 50 wt.%. A borosilicate

* Corresponding author.
E-mail addresses: safronova@inorg.chem.msu.ru (T.V. Safronova), putl@inorg.chem.msu.ru (V.I. Putlyaev), shekhirev@gmail.com (M.A. Shekhirev), yudt@inorg.chem.msu.ru (Y.D. Tretyakov), ant2121kuz@rambler.ru (A.V. Kuznetsov), av_bel@bk.ru (A.V. Belyakov).

0955-2219/$ – see front matter © 2008 Elsevier Ltd. All rights reserved.
doi:10.1016/j.jeurceramsoc.2008.12.012

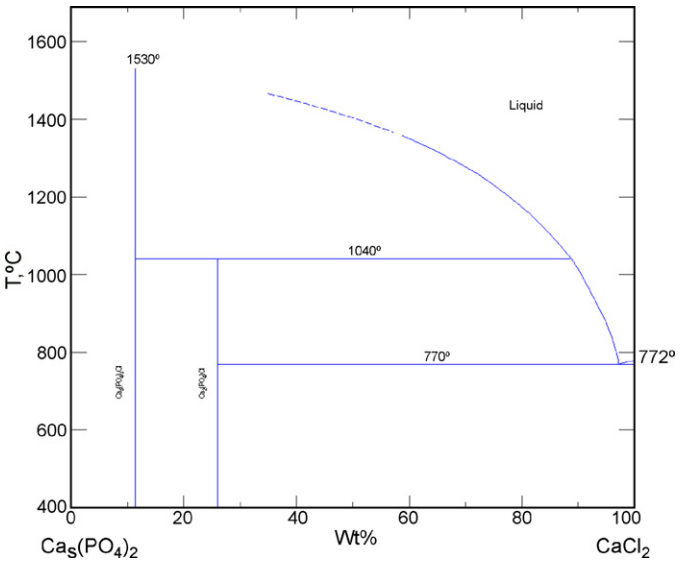

Fig. 1. Phase diagram $CaCl_2$–$Ca_5(PO_4)_3Cl$ for the $CaCl_2$–$Ca_3(PO_4)_2$ system.[20]

glass in an amount of 50% was also tested as a sintering additive.[18] In the case of biocompatible HAp-based ceramics, components constituting the additive should either be present in natural bones or belong to the group of bioinert materials. Note, however, that in most cases of the liquid-phase sintering, the concomitant formation of tricalcium phosphate (TCP) or CaO occurs. The presence of TCP is not crucial for biomedical purposes. Meanwhile, if CaO is present in ceramics, it readily reacts with water to yield $Ca(OH)_2$, which can give rise to undesirable changes in pH *in vivo*. Furthermore, this reaction induces volume changes and the resultant mechanical stresses can give rise to microcracking thus decreasing the strength of the target material.

A prominent trend in the development of structural ceramics (*e.g.*, Al_2O_3-based) consists of the search for the preparation conditions, which would enable a decrease in the sintering temperature (down to 1450 °C in the case of alumina) not compromising the strength of the target material, in particular, using appropriate advanced sintering additives.[19] For the densification driven by the formation of an eutectic melt, it is possible to use either an additive of the eutectic composition or a compound, which is capable of reacting with powder grains of the main phase to afford an eutectic melt. To adapt the strategy mentioned above to the sintering of HAp, it seems promising to explore the $Ca_{10}(PO_4)_6Cl_2$ (chlorapatite, hereinafter referred to as ClAp)–$CaCl_2$ system, which is characterized by an eutectic point of about 750 °C (Fig. 1).[20] This means that the reaction of calcium chloride (acting as an additive to HAp powder) with HAp shifts the overall composition of the sample, located inside the triangle HAp–ClAp–$CaCl_2$ in the vicinity of HAp corner, toward the ClAp–$CaCl_2$ side. In order to overcome the problem of a possible collapse of the apatite structure due to the reaction with $CaCl_2$ excess leading to a formation of chlorspodiosite, $Ca_2(PO_4)Cl$,[21] at $T \leq 1040$ °C, Ca-deficient HAp (CDHAp) should be used as a starting material. It is believed that Ca vacancies are filled with extra Ca atoms coming from the sintering additive according to the summary process (not reflecting details of the transformation):

$$Ca_{10-x}(HPO_4)_x(PO_4)_{6-x}(OH)_{2-x} + xCaCl_2 = Ca_{10}(PO_4)_6(OH)_{2-x}Cl_x + xHCl\uparrow .$$

Calcium chloride was tested as a sintering additive earlier.[13] However, this trial was unsuccessful, likely due to its small amount (*ca.* 5%) and a non-uniform distribution over the sample. Consequently, in order to observe the effect of a liquid-phase formation, we have chosen to increase the quantity of this additive up to 10 wt.% (or 12 vol.%), being the lowest limit for the complementary CDHAp (the reaction above needs then *ca.* 12 vol.% of $CaCl_2$ for the CDHAp with Ca/P = 1.5; note, however, that this amount does not meet the percolation threshold for a liquid phase exceeding 16 vol.%). As has been shown elsewhere,[22] the crystallization of HAp from $CaCl_2$ melts proceeds rather sluggishly and does not yield whiskers (*i.e.*, only crystals with small aspect ratios are formed), which implies that the presence of $CaCl_2$ induces the formation of nearly isotropic particles. From the viewpoint of ceramics microstructure development, the formation of virtually equiaxed particles may be regarded as a positive result. It means that the $CaCl_2$ melt interacts with nanosized HAp particles (100 nm) by the sequential "dissolution-crystallization-growth" mechanism providing the growth of HAp grains up to 200 μm for 3 h at 850–1000 °C and selectively inhibiting the growth along the *c*-axis owing to efficient wetting of the basal faces of HAp grains. The present work is aimed at the elucidation of the role played by NH_4NO_3 (a by-product of the solution synthesis of HAp) and $CaCl_2$ in the densification of nanosized HAp powder in the course of the conventional sintering. It is of note that significant amount of NH_4NO_3 captured by HAp precipitate can be removed (and this is commonly held step in HAp preparation) by washing the precipitate with water. Here, we report on the HAp powder obtained without this washing with water-step.

2. Experimental

2.1. Powder synthesis and samples preparation

HAp powder samples were fabricated via conventional wet-precipitation technique by a dropwise addition of an $(NH_4)_2HPO_4$ solution (0.15–1.00 M) to a starting solution of $Ca(NO_3)_2$ (0.25–1.67 M) with a pre-adjusted pH at 60 °C. The pH of the mixture was maintained at a constant value (about 9 and 7) by addition of appropriate amounts of NH_4OH. The solution was vigorously stirred. After addition of the specified amount of the $(NH_4)_2HPO_4$ solution, the suspension was matured for 30 min and then filtered without washing. The resulting precipitate was dried at room temperature for 48 h. Dry powder was disaggregated in a ball mill for 3 min in acetone or alcohol media with a liquid: powder: balls proportion set to 2:1:3. A surplus of $CaCl_2$, in amount of 10 wt.% to a powder charge, was added at the stage of disaggregating (alcohol media, ratio liquid:powder:balls = 1:1:3, 3 min). The powder processed in this way was sieved (Saatilene HiTechTM polyester fabrics, cells of 200 μm). The samples (charges of about 0.5 or 1.5 g,

without plasticizer) were uniaxially compacted in a stainless steel mold into 5 mm × 10 mm or 6 mm × 40 mm rectangular bars at 50 MPa. The powder and compacted samples were then annealed at 1100 °C. To reveal a microstructure, the samples were polished with diamond pastes (down to 1 μm) and the silica suspension (OP-S with grain size less than 1 μm, Struers, Denmark), and then thermally etched at 900–1000 °C for 30 min.

2.2. Samples characterization

Densities of the green compacts and sintered samples were determined by geometrical measurements assuming a theoretical density of 3.156 g/cm^3 for HAp. XRD patterns were obtained with Co Kα radiation using a DRON-3M powder diffractometer (Russia). FTIR spectra of the powders were recorded on a PE-1600 FTIR spectrometer (PerkinElmer, USA) in the range of 400–4000 cm^{-1} with a scanning step of 4 cm^{-1}. TGA of the specimens was conducted with a Diamond Pyris apparatus (PerkinElmer, USA) in air up to 1000 °C at a heating rate of 10 °C/min. The linear shrinkage of compacts was determined with a NETZSH 402 dilatometer at a ramp rate of 10 °C/min and a LIR-1400 dilatometer (Russia) at a ramp rate of 5 °C/min. For these measurements, the bar-shaped samples of 6 mm × 4 mm × 10 mm were heated in air up to 1000 °C. The microstructure of the powders and dense specimens was elucidated using FESEM with a LEO Supra 50 VP scanning electron microscope (Carl Zeiss, Germany) operated at 5–10 kV and TEM with a JEM-2000 FXII transmission electron microscope (JEOL, Japan) operated at 200 kV. The chemical composition of the samples (Ca/P ratio) was determined using an EDX attachment (INCA Energy +, Oxford Instruments, UK) to the LEO Supra 50 VP electron microscope.

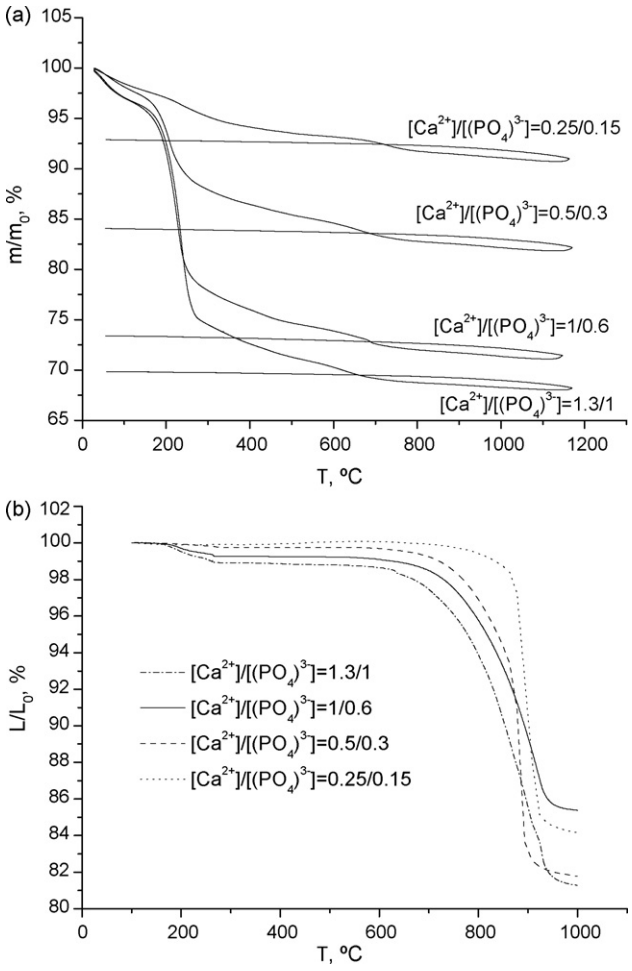

Fig. 2. TGA of the HAp powders (a) and linear shrinkage curves for the compacts fabricated from the HAp powders with Ca/P = 1.67 (b).

3. Results and discussion

According to XRD, all as-synthesized powders consist of NH_4NO_3 and nanocrystalline HAp (the crystallite sizes estimated from the diffraction peak broadening and TEM micrographs lie in the range of 15–40 nm) with a Ca/P ratio close to 1.67, according to the EDX data. In addition to the apatite phase, the presence of a significant amount of NH_4NO_3 in the dry powders was revealed by FTIR (a pronounced band at 1380 cm^{-1}). Its fraction varies from 5.73 to 27.40% (Table 1, Figs. 2a and 3a), as determined from the TGA-curves (a mass loss in the temperature range of 20–400 °C, since NH_4NO_3 decomposes at 210 °C) and the mass gains of the precipitates with respect to the theoretical yields. It was found that the density of green compacts increases with increasing concentration of the starting solutions. The measured densities lie within 39–42% of the theoretical value with the maximum density achieved for the sample fabricated from the most concentrated solution. It would be reasonable to attribute this trend to a decrease in the size of HAp crystals with simultaneous increase in the size of their aggregates (evidenced by SEM) as concentration of the solutions increases.

Table 1
Synthesis conditions and powder characteristics.

Synthesis condition				Mass loss 400 °C (%)	Starting powder density (g/cm^3)	Compacted powder density (P = 50 MPa) (%)
$c(Ca^{2+})$ (M)	$c(PO_4^{3-})$ (M)	Ca/P ratio	pH			
0.25	0.15	1.67	9	5.87	0.28	39
0.5	0.3	1.67	9	13.55	0.36	40
0.5	0.3	1.67	7	5.73	0.42	40
0.5	0.3	1.61	7	7.68	0.51	43
0.5	0.3	1.48	7	8.29	0.31	39
1.0	0.6	1.67	9	23.99	0.42	42
1.6	1.0	1.67	9	27.40	0.40	46

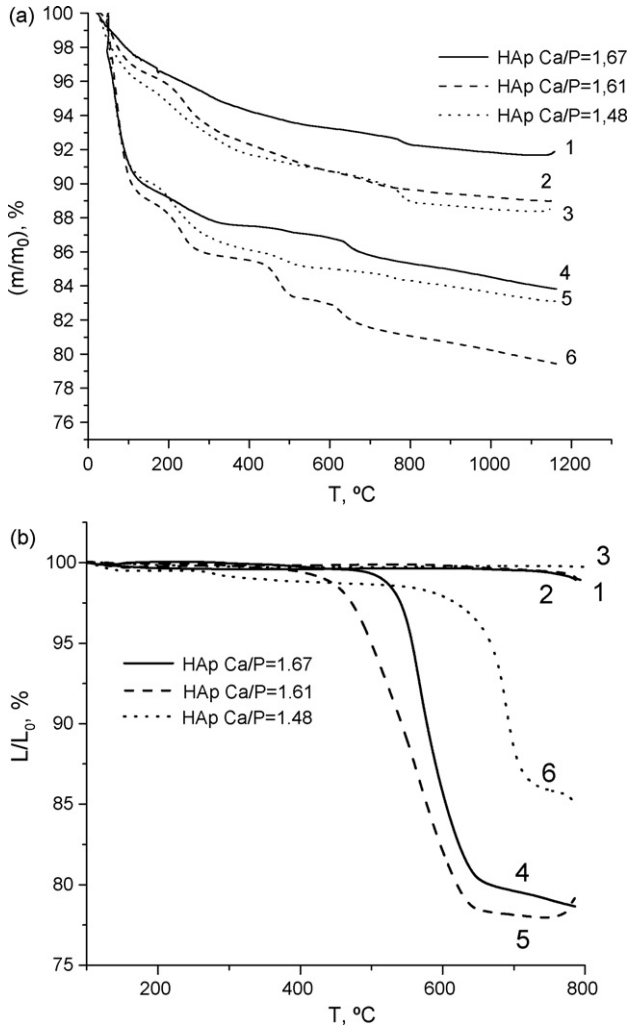

Fig. 3. (a) TGA of the HAp powders, and (b) linear shrinkage curves for the compacts fabricated from the HAp powders with different Ca/P ratios and $[Ca^{2+}] = 0.5$ M: without additive (curves 1–3) and with 10% of $CaCl_2$ (curves 4–6).

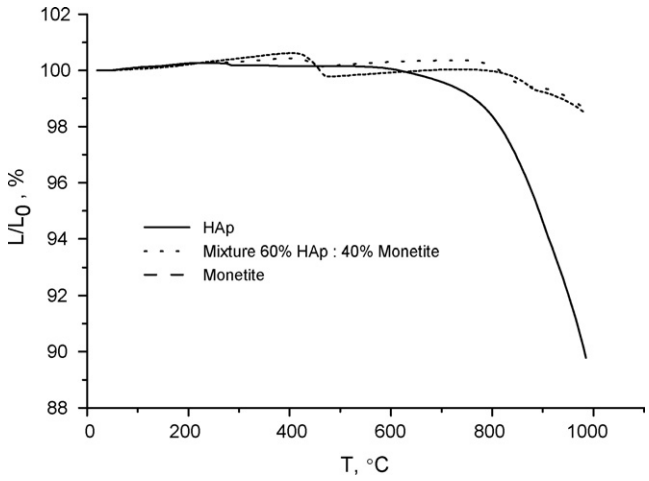

Fig. 4. Linear shrinkage curves for the compacts fabricated from monetite (Ca/P = 1) powder, HAp (Ca/P = 1.67) powder and mixture of HAp (Ca/P = 1.67)/monetite (Ca/P = 1) synthesized from the solution with $[Ca^{2+}] = 0.5$ M.

According to dilatometry measurements (Figs. 2b and 3b), NH_4NO_3 performs as a densification additive for stoichiometric HAp (Ca/P = 1.67), since it undergoes melting in the temperature range of 150–250 °C. The shrinkages starting at 150–250 °C are attributable to the NH_4NO_3 melting, which is accompanied by the actuation of capillary forces and surface tension in pores of the compact. This promotes the formation of primary contacts between particles and evokes their rearrangement rendering the initial structureless compact into a granular porous body. At higher temperatures, NH_4NO_3 starts to decompose, which is accompanied by the liberation of gaseous N_2O and water from the porous body. The shrinkages at 700–950 °C are related to the pore curing and grain growth, which represents essentially solid-state sintering of HAp ceramics. The maximum linear shrinkage rate for one of the synthesized HAp powder samples (Ca/P = 1.67, pH 9) is observed at 850–950 °C. In the case of green compacts prepared from more concentrated solutions, which are thus characterized by smaller HAp crystals, the densification starts at a lower temperature and proceeds more smoothly. Meanwhile, abrupt shrinkage in a narrow temperature range occurs for the samples prepared from dilute solutions.

TGA measurements showed that an increase in the concentration of the solutions gives rise to a larger adsorption of the NH_4NO_3 by-product by the HAp precipitate from the mother liquor (Fig. 2a). A decrease in the Ca/P ratio for the HAp sample precipitated at pH 7 can be explained by a change in the composition of the adsorbing layer due to the presence of extra phosphate ions in the solution. Upon annealing, the surplus PO_4^{3-} can react with the main phase, by-product and the additive thus affecting the overall sintering process. In the case of Ca^{2+} deficit, the formation of calcium phosphates other than HAp is possible. The samples containing the $CaCl_2$ additive demonstrate virtually linear mass loss above 750 °C. This change can be attributed to the HCl liberation from the compact due to the high-temperature hydrolysis of hydrated $CaCl_2$ (according to the reaction $2CaCl_{2(cr)} + H_2O_{(g)} = 2HCl_{(g)} + Ca_2OCl_{2(cr)}$[1] driven largely by entropy factor). It is also possible that calcium chloride and oxychloride efficiently evaporate at higher temperature. In principle, $CaCl_2$ additive can be completely removed from ceramics at the end of sintering owing to the hydrolysis and evaporation, and these processes can be accelerated by sintering in an atmosphere saturated with water vapor.

The shrinkage curves for HAp powders with various Ca/P ratios fabricated at pH 7 indicate that the sintering process starts above 800 °C (Fig. 3b). This agrees fairly well with the results of a dedicated experiment on the sintering of compacts composed of HAp (obtained at pH 9; Ca/P = 1.67), $CaHPO_4$ or their mixture (HAp:$CaHPO_4$ = 60:40 wt.%). Two latter samples underwent shrinkages at temperatures just above 800 °C, whereas pure HAp starts to sinter at 600 °C (Fig. 4). Such a behavior demonstrates a crucial effect of pyrophosphate parti-

[1] Calcium oxychlorides Ca_4OCl_6[24] and Ca_5OCl_8[25] are also described. However, variation of a composition of the oxychloride does not affect generality of considerations made in this article.

Table 2
Thermodynamic data for the reactions occurring in HAp–TCP–$CaCl_2$ mixture (calculated on the base of values borrowed from[25,31–33]).

No.	Equation of the reaction	$\Delta_r H^\circ_{298}$(kJ)	$\Delta_r S^\circ_{298}$(J K^{-1})	Thermal conditions for $\Delta_r G^\circ < 0$
1	$3TCP_{(cr)} + CaCl_{2(cr)}$[a] $= ClAp_{(cr)}$	−103.3	12.2	at any T
2	$3TCP_{(cr)} + CaO_{(cr)} = OAp_{(cr)}$[b]	−78.8	1.2	at any T
3	$OAp_{(cr)} + CaCl_{2(cr)} = ClAp_{(cr)} + CaO_{(cr)}$	−24.5	11.0	at any T
4	$OAp_{(cr)}$[b] $+ H_2O_{(g)} = HAp_{(cr)}$	−159.5	−152.6	$T \leq 770\,^\circ$C
5	$ClAp_{(cr)} + H_2O_{(g)} = OAp_{(cr)} + 2HCl_{(g)}$	−242.7	126.6	at any T
6	$ClAp_{(cr)} + 2CaCl_{2(cr)} = 6Ca_2(PO_4)Cl_{(cr)}$	? (>0)[c]	? (>0)[c]	$T \leq 1040\,^\circ$C

Notes: TCP = $Ca_3(PO_4)_2$ (tricalcium phosphates), HAp = $Ca_{10}(PO_4)_6(OH)_2$ (hydroxyapatite), ClAp = $Ca_{10}(PO_4)_6Cl_2$ (chlorapatite), OAp = $Ca_{10}(PO_4)O$ (oxyapatite).

[a] In the case of a melt (*i.e.*, $CaCl_{2(lq)}$) one has to subtract the enthalpy of fusion $\Delta_{fus}H^\circ = 28.0$ kJ mol^{-1} and the entropy of fusion $\Delta_{fus}S^\circ = 26.8$ J mol^{-1} K^{-1} from the corresponding thermodynamic functions; formation of the melt does not change spontaneous character of the reaction (1) at any reasonable temperature.

[b] At temperature higher than 770 °C in accordance with the reaction (4), HAp begins to evolve water forming mixed oxy-hydroxyapatite $Ca_{10}(PO_4)_6O_{x/2}(OH)_{(1-x)}$; oxyapatite (OAp–$Ca_{10}(PO_4)_6O$) as an apatite-like phase without any trace of trace of water exists temperature higher than 1100 °C. Specifying OAp in all transformations below 1100 °C mentioned in this table and Fig. 6 has the aim to express the direction of changing of HAp composition as temperature increases, it does not affect generality of considerations made in the text. Also, thermodynamic data on oxy-hydroxyapatite are not available.

[c] Signs of the enthalpy and the entropy of the reaction (6) can be deduced from the fact of incongruent melting of chlorspodiosite, $Ca_2(PO_4)Cl$, as it follows from a phase diagram of the $CaCl_2$–ClAp system.[20]

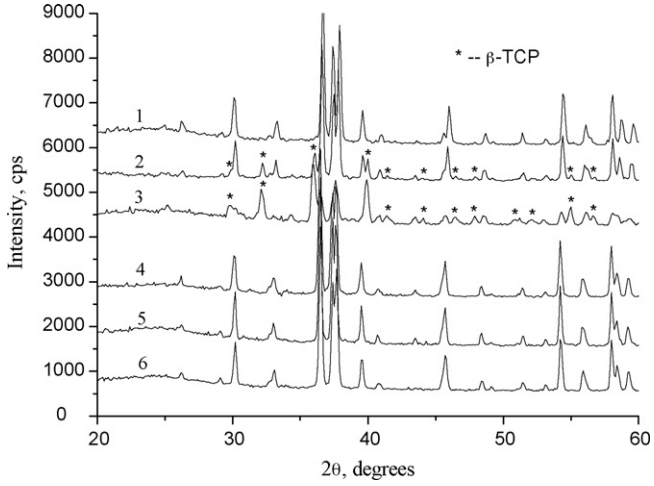

Fig. 5. XRD patterns of the HAp ceramics (1100 °C, 6 h) fabricated from the powders synthesized at different Ca/P ratios and [Ca^{2+}] = 0.5 M: without additive (curves 1–3) and with 10% of $CaCl_2$ (curves 4–6).

cles produced by the $CaHPO_4$ decomposition at early stages of the densification.[2] This issue was partially addressed by Raynaud et al. in a study,[6] where a $CaHPO_4$ admixture was detected by means of XRD in HAp powders precipitated from solutions with Ca/P < 1.5. In another study,[23] it was shown that pyrophosphate particles (produced from brushite via monetite) preserved their plate-like shape upon annealing. In our case, the XRD patterns of HAp with different Ca/P ratios synthesized at pH 7 and annealed at 1100 °C or above (Fig. 5) indeed revealed TCP admixtures originating from the solid-state reaction of HAp with other calcium phosphates with smaller Ca/P ratios (viz., Ca/P = 1 for brushite, monetite, and pyrophosphate). This again confirms the dramatic influence of the presence of pyrophosphate crystals with the plate morphology produced from monetite even in the case of a large HAp excess.

According to the shrinkage curves, the maximum linear shrinkage rate for all the samples containing $CaCl_2$ (Fig. 3b) occurs in the temperature range of 450–700 °C. We can expect that the presence of the $CaCl_2$ additive, which is characterized by the melting point of 772 °C, indeed induces the formation of a melt (or an eutectic melt) at a temperature lower than 772 °C. Taking this supposition as a starting point as well as the fact that the presence of calcium pyrophosphate causes the production of TCP and the possibility of the reactions (1)–(3) (Table 2), we can suggest that the $CaCl_2$ additive should form an eutectic melt with Cl-apatite. The occurrence of these reactions (viz., the reaction (3)) means that the molten additive promotes the transformation of HAp to ClAp, more stable apatite phase at high temperature. Although the reactions (1)–(3) listed in Table 2 are thermodynamically possible at any temperature, their kinetics seems to be controlled by the amount of a liquid phase originated from the eutectic melting. Thus, the reactions (1)–(3) represent the source of the melt (ClAp + $CaCl_2$), and the reactions (5) and (6) describe how the melt can be digested. Phase transformations briefly discussed above are summarized in the form of a flow chart (Fig. 6). It is important that flows in the chart are terminated by HAp, that is, the only target phase for these transformations is apatite (this conclusion is also supported by spectra 4–6 in Fig. 5).

Therefore, we can expect that the $CaCl_2$ additive, after melting, wetting and densification, is incorporated into the (micro)structure of apatite ceramics. The fact that the sintering starts at a temperature below the eutectic melting in the $CaCl_2$–ClAp binary system (*e.g.*, 450 °C for HAp synthesized at pH 7 and Ca/P = 1.61 *vs.* 500 °C for HAp synthesized at pH 7 and Ca/P = 1.67) means that a metastable equilibrium involving the formation of a liquid can exist in this system. The shrinkage curve for the HAp sample synthesized at pH 7 and Ca/P = 1.61 reveals a plateau at 650 °C corresponding to a shrinkage of 22%. Meanwhile, the HAp samples fabricated at pH 7 and Ca/P = 1.67 demonstrate smaller shrinkages of *ca.* 19–20%, and the sample with Ca/P = 1.48 – the smallest shrinkage of 15% in the

[2] Another source of a pyrophosphate phase is the partial decomposition of CDHAp, $Ca_{10-x}(HPO_4)_x(PO_4)_{6-x}(OH)_{2-x}$, in accordance with the scheme: $2HPO_4^{2-} \rightarrow P_2O_7^{4-} + H_2O$. Pyrophosphate ions in a calcined CDHAp can be discovered by several analytical techniques (see for details, e.g.[26]).

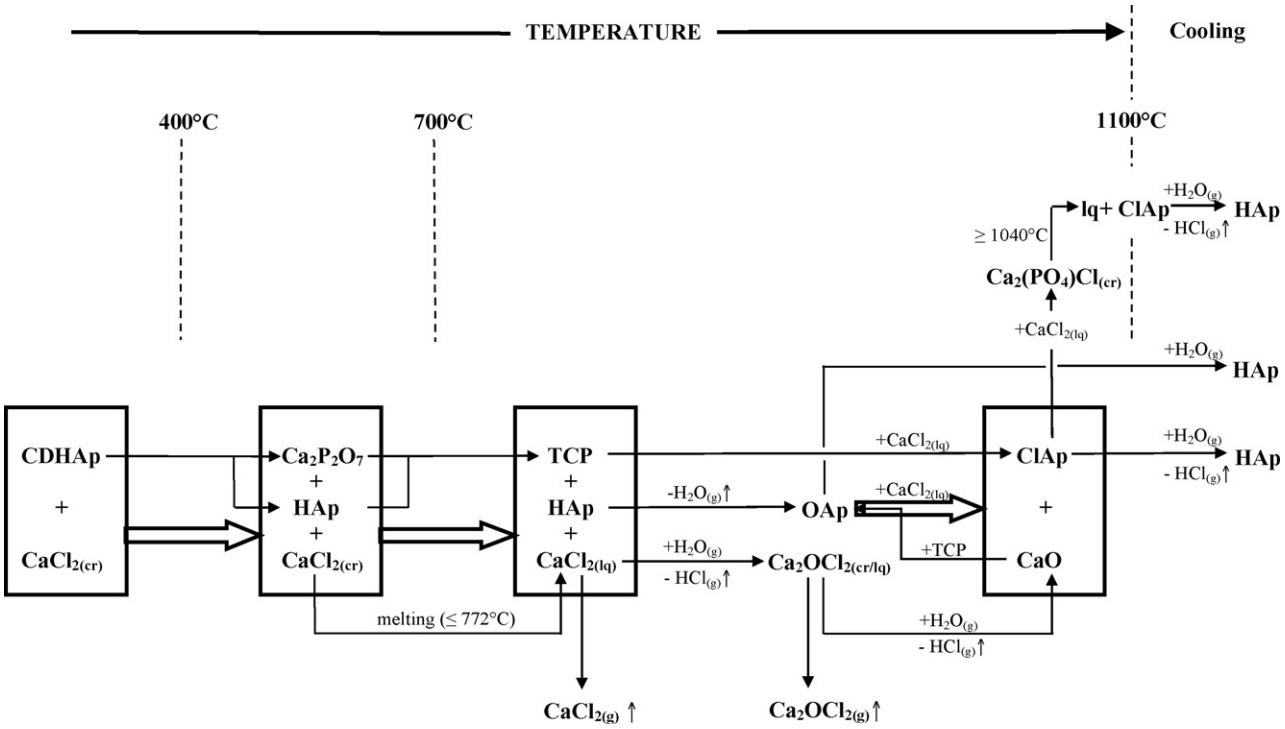

Fig. 6. Phase transformations in the HAp ceramics under study (note that at temperatures lower than 1100 °C, mixed oxy-hydroxyapaite $Ca_{10}(PO_4)_6O_{x/2}(OH)_{(1-x)}$ forms, rather than OAP; see the note to Table 2 for details).

temperature range from 450 to 800 °C. Swelling phenomenon, clearly visible after 750 °C as expansion of the sample (curve 6 in Fig. 3b), is also worth mentioning.

The facts above can be rationalized by general regularities of liquid-phase sintering. Since the liquid content is less than required for pore filling, all stages of densification, proper to liquid-phase sintering (*i.e.*, particle rearrangement, solution-reprecipitation and solid skeleton sintering), take place.[27] Fast densification occurring in the interval from 450 to 600 °C should be attributed largely to particle rearrangement events controlled by heat transfer. Solution-precipitation phenomena (slower processes compared to the previous one) contribute to the overall shrinkage and limit the rate of densification around 600 °C. It should be outlined that (a) solid solubility in liquid, and (b) liquid solubility in solids, are the key factors governing densification in the course of the sintering. The former of these leads to extensive densification due to liquid production (the reactions (1)–(3) in our case) accompanied by grain shape accommodation, while the later one causes swelling because of liquid consumption (according to the reactions (5) and (6)) resulting in pore formation. Swelling becomes predominant and retard densification after 600 °C as it is evidenced by the presence of the plateau and even expansion of the samples (curve 5 and 6, Fig. 4). Thereupon, it is reasonable to speculate that extensive swelling, arising from significant consumption of the liquid phase for the sample with Ca/P = 1.48, is responsible for the low value of observed shrinkage in this case (curve 4, Fig. 3b).

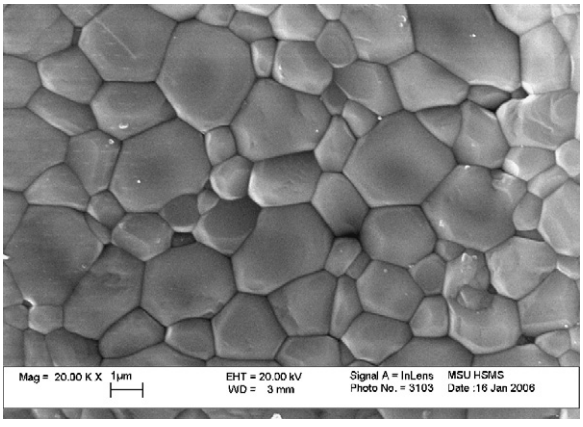

Fig. 7. SEM micrographs of the HAp ceramics (pH 9, Ca/P = 1.67) annealed at 1200 °C for 6 h.

According to the electron microscopy study, the microstructure of HAp ceramics synthesized at pH 9 and Ca/P = 1.67 and annealed at $T = 1100$ °C does not correspond to complete sintering. Dense HAp ceramics (with a density on the order of 94–96% of the theoretical value and the mean grain size of about 1.5 μm) is produced only upon annealing at 1200 °C (Fig. 7). The sintering of the HAp powder fabricated at pH 7 and Ca/P = 1.67 at $T = 1100$ °C yield rather dense material with a bimodal size distribution of grains (1 μm/300 nm). It is of note that TCP is present in sufficient amount (up to 50%) in this sample, according to XRD (Fig. 5). A decrease in the mean grain size in calcium phosphate-based ceramics (pH 7) with respect to that in HAp-based ceramics is due to the lower sintering temperature and a possibility of the solid-state reaction yielding TCP therein. Alternatively, this can be due to the decomposition or other solid-state reactions of non-stoichiometric HAp, which is typically afforded at pH 7, with other calcium phosphates with Ca/P < 1.67, which are preferable formed at pH ≤ 7.

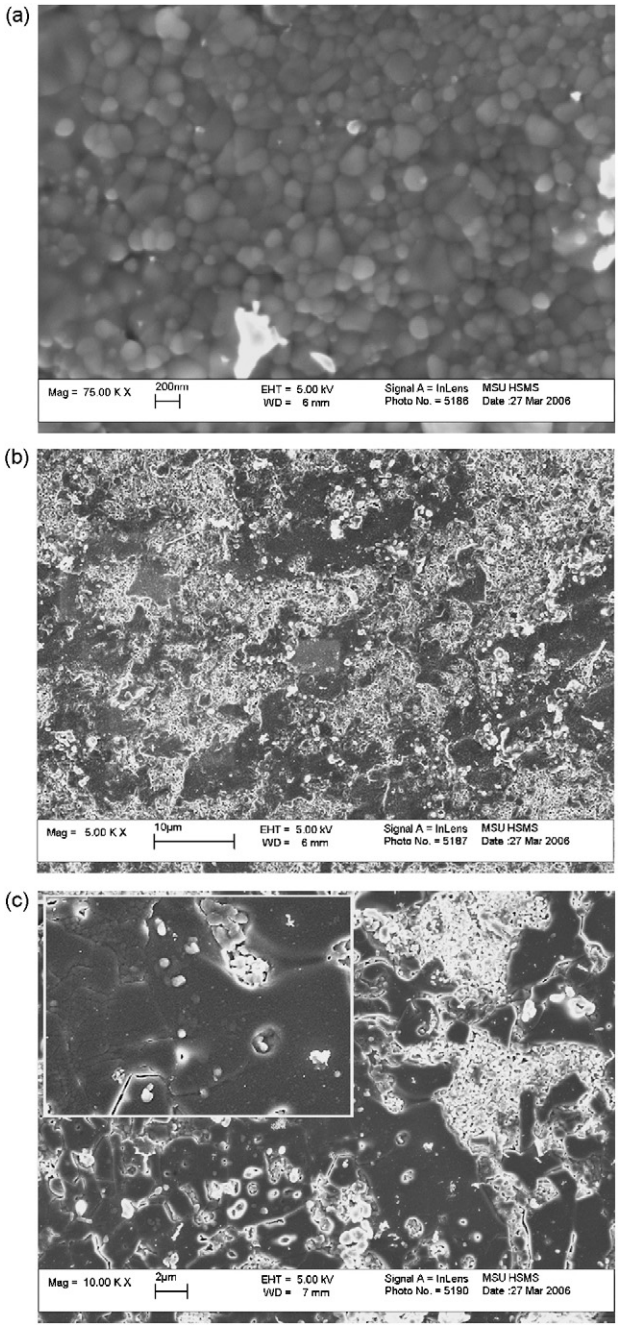

Fig. 8. SEM micrographs of the HAp ceramics (pH 7, Ca/P = 1.67) annealed at 1100 °C for 6 h with $CaCl_2$ (a and b); the sample of the ceramics (pH 7 and Ca/P = 1.67), with $CaCl_2$, after dilatometry terminated at 1000 °C (the lower right corner of the inset marks the center of twofold magnified region) (c).

The effect of the $CaCl_2$ additive on the ceramics microstructure is illustrated in Fig. 8. Three features are specific for these micrographs.

(i) Significant portion of examined areas in the samples doped with $CaCl_2$ is dominated by grains not exceeding 200 nm (Fig. 8a). The grains grew nearly fivefold with respect to the size of individual crystallites in the starting powder during the sintering. Both unmodified HAp- (pH 9, 1200 °C) and HAp/TCP-based ceramics (pH 7, 1100 °C) demonstrated more pronounced grain growth upon sintering. As it has been established within the studies of clinker formation, metal chlorides, including $CaCl_2$, decrease the interface energy in oxide melts thus acting as high-temperature surfactants.[28] Note that a real mechanism retarding grain growth may differ from just wetting of grains with a melt. A peritectic reaction of the type (6) (see Table 2 and Fig. 6) leads to covering of grains with a crystalline shell of the chlorspodiosite, $Ca_2(PO_4)Cl$. The spodiosite shell decreases a diffusion flux of Ca^{2+}, PO_4^{3-}, and Cl^- ions from the melt to the ClAp/chorspodiosite interface in the direction normal to grain surface, thus inhibiting grain growth. At the same time, grain shape accommodation evidenced by rounded shape of well-fitted particles (Fig. 8a) is indicative of solution-reprecipitation events in the course of liquid-phase sintering,[29] which are responsible for effective densification. However, the amount of liquid seems to be not enough to cause significant Ostwald ripening of the particles. Therefore, the microstructure discussed above manifests a transient state of sintering from liquid-phase to solid-state (solid skeleton) regime.

(ii) Importantly, this study was not focused on the optimization of the additive amount and sintering parameters. Due to this reason, the HAp-based material (Ca/P = 1.67, 1100 °C) reveals non-uniform microstructure with prominent nanostructured and coarser microstructured domains in an image corresponding to a lower magnification and a larger view field (Fig. 8b). The microstructure becomes more heterogeneous including extended fine-grain porous domains as the Ca/P stoichiometry decreases from 1.67 to 1.48. So yet another reason for a duplex microstructure accompanied by development of porosity in the fine-grain regions can be consumption of the melt according to the reactions (5) and (6) (Table 2, Fig. 6). The tendency in evolution of the microstructure reported here agrees fairly well with the shrinkage behavior of the samples discussed earlier.

(iii) It is surprising, at first sight, that the HAp-based material (pH 7, 1000 °C without prolonged annealing after dilatometry) consists of large grains with a size on the order of 10–20 μm (Fig. 8c). Presumably, these grains are constituted of nanoparticles bound into blocks by chlorspodiosite interlayers and the remaining melt, which is completely removed from the material upon annealing at a higher temperature due to either evaporation or temperature-assisted hydrolysis of $CaCl_2$. Heating the ceramics over 1040 °C leads to peritectic melting of the $Ca_2(PO_4)Cl$ layers. Then the amount of liquid increases, the melt penetrates through the pores and grain boundaries by a combination of reaction and capillarity, causing fragmentation of the blocks into primary particles. Afterward secondary rearrangement of the particles and solution-reprecipitation events take place. Thus, a grain size of the ceramics sintered at temperature higher than 1040 °C can be even less than that for the ceramics fired at lower temperature. This is consistent with the observation of non-monotonous coarsening of HAp crystallites with $CaCl_2$ surplus in the region of 1000–1100 °C for powdered samples.[30]

4. Conclusion

NH_4NO_3 can act as an additive forming a liquid at relatively low temperatures (150–250 °C) prior to incongruent evaporation from the compact. It enables particles to rearrange in a way to realize a more dense packing at the very beginning of sintering. Furthermore, the addition of $CaCl_2$ positively affects the powder compaction by lowering the densification temperature. For pure nanocrystalline HAp powder (Ca/P = 1.61, pH 7), the addition of $CaCl_2$ makes it possible to achieve 22% of the total linear contraction already at a temperature as low as 450 °C, and the densification is eventually completed at 650 °C. Several mechanisms of the $CaCl_2$ action as a densification additive might be envisaged: (i) the formation of a low-temperature melt; (ii) the wetting of grain surface; (iii) a change in the growth morphology due to the high-temperature surfactant properties; (iv) a reaction with the HAp phase on the surface of grains giving rise to the HAp decomposition and the formation of the intermediate phases related to ClAp.

Acknowledgements

This work was partially supported by the Federal Program 'R&D for priority directions of science and technology in Russia for the period of 2007–2012 years' (topic 1.3, code 2007-3-1.3-24-02-004, Federal Contracts #02.513.11.3159, #02.513.11.3160, and #02.513.12.3008). RFBR funding is also acknowledged (grants #07-08-00576, 09-03-01078).

The assistance of M. Akhmedov in preparing the manuscript, Dr. N. Lyskov in TGA-experiments, Dr. R. Muydinov and Dr. I. Archangelskiy in dilatometry is deeply appreciated.

References

1. Gibson, I. R. and Bonfield, W., Method for preparation of carbonated hydroxyapatite compositions. US Patent 6,582,672, 2003.
2. Bonfield, W. and Gibson, I. R., Process for the preparation magnesium and carbonate substituted hydroxyapatite. US Patent 6,585,946, 2003.
3. Best, S., Bonfield, W., Gibson, I. R. and Lee, J. L., Silicon-substituted apatites and process for the preparation thereof. US Patent 6,312,468, 2001.
4. Kim, S. R., Synthesis of Si, Mg substituted hydroxyapatite and their sintering behaviors. *Biomaterials*, 2003, **24**, 1389–1398.
5. Ito, A., Ichinose, N., Ojima, K., Layrolle, P. and Kawamura, H., Zinc-doped tricalcium phosphate ceramic material. US Patent 6,090,732, 2000.
6. Raynaud, S., Champion, E., Bernache-Assollant, D. and Thomas, P., Calcium phosphate apatites with variable Ca/P atomic ratio: I. Synthesis, characterisation and thermal stability of powders. *Biomaterials*, 2002, **23**, 1065–1072.
7. Raynaud, S., Champion, E., Bernache-Assollant, D. and Thomas, P., Calcium phosphate apatites with variable Ca/P atomic ratio: II. Calcination and sintering. *Biomaterials*, 2002, **23**, 1073–1080.
8. Strelov, K. K., Kachzeev, I. D. and Mamykin, P. S., *Tekhnologiya Ogneuporov (Technology of Refractories)*. Metallurgia, Moscow, 1988, p. 528 [in Russian].
9. Budnikov, P. P. and Poluboyarinov, D. N., *Khemicheskaya tekhnologiya keramiki i ogneuporov (Chemical Technology of Ceramics and Refractories)*. Stroyizdat, Moscow, 1972, p. 552 [in Russian].
10. Kukolev, G. V. and Leve, E. N., Issledovanija processa spekaniya glinozema v razlichnykh sistemakh (Investigations of sintering process of alumina in different systems). *Zhurnal Prikladnoy (Russian J. Appl. Chem.)*, 1955, **28**(8), 807–816 [in Russian].
11. Makarov, N. A., Use of additives forming liquid phase in firing in corundum ceramics technology (a review). *Glass Ceram.*, 2003, **60**(9–10), 334–338 [translated from Russian].
12. Chiang, Y.-M. and Birnie III, D., *Kingery, Physical Ceramics: Principles for Ceramic Science and Engineering*. Wiley, New York, 1997, p. 544.
13. Suchanek, W., Yashima, M., Kakihana, M. and Yoshimura, M., Hydroxyapatite ceramics with selected sintering additives. *Biomaterials*, 1997, **18**, 923–933.
14. Takami, A. and Kondo, K., Phosphate of calcium ceramics. US Patent 4,308,064, 1983.
15. Safina, M. N., Safronova, T. V. and Lukin, E. S., Calcium phosphate based ceramic with a resorbable phase and low sintering temperature. *Glass Ceram.*, 2007, **64**(7–8), 19–24 [translated from Russian].
16. Georgiou, G. and Knowless, J. C., Glass reinforced hydroxyapatite for hard tissue surgery: Part 1. Mechanical properties. *Biomaterials*, 2001, **22**, 2811–2815.
17. Tancred, D. C., McCormack, B. A. O. and Carr, A. J., A quantitative study of sintering and mechanical properties of hydroxyapatite/phosphate glass composites. *Biomaterials*, 1998, **19**, 1735–1743.
18. Hu, Y. and Miao, X., Comparison of hydroxyapatite ceramics and hydroxyapatite/borosilicate glass composites prepared by slip casting. *Ceram. Int.*, 2004, **30**, 1787–1791.
19. Belyakov, A. V., Lukin, E. S. and Makarov, N. A., *Evolution of Structure in Sintering Ceramics Based on Aluminum Oxide with a Eutectic Additive*. Springer, New York. Glass Ceram. 2002, **59**(3–4), 127–131.
20. Nacken, R., *Zentralbl. Mineral. Geol. Palaeontol.*, 1912, 545–559.
21. Greenblatt, M., Banks, E. and Post, B., The crystal structures of the spodiosite analogs, Ca_2CrO_4Cl and Ca_2PO_4Cl. *Acta Crystallogr.*, 1967, **23**(1), 166–171.
22. Cuneyt Tas, A., Molten salt synthesis of calcium hydroxyapatite whiskers. *J. Am. Ceram. Soc.*, 2001, **84**(2), 295–300.
23. Cuneyt Tas, A., Chemical processing of $CaHPO_4{\cdot}2H_2O$: its conversion to hydroxyapatite. *J. Am. Ceram. Soc.*, 2004, **87**(12), 2195–2200.
24. Meyer, H.-J., Meyer, G. and Simon, M., An oxide chloride of calcium, Ca_4OCl_6. *Z. Anorg. Allg. Chem.*, 1991, **596**, 89–92.
25. Bogach, V. V., Dobridnev, S. V. and Beskov, V. S., Calculation of thermodynamic properties of apatites. *Zh. Neorg. Khimii*, 2001, **46**(7), 1127–1131 [in Russian].
26. Wilson, R., Elliot, J. and Dowker, S., Rietveld refinements and spectroscopic studies of the structure of Ca-deficient apatite. *Biomaterials*, 2005, **26**, 1317–1327.
27. Barsoum, M. W., *Fundamentals of Ceramics*. IOP Publishing, Bristol and Philadelphia, 2003, pp. 337–342.
28. Osokin, A. P. and Potapova, E. N., Composition, structure, and properties of oxide-salt melts. *Glass Ceram.*, 2003, **60**(9–10), 296–301 [translated from Russian].
29. German, R. M., *Liquid Phase Sintering*. Plenum Press, NY, 1985.
30. Stepuk, A. A., Veresov, A. G., Putlyaev, V. I. and Tret'yakov, Yu. D., The influence of NO_3^-, CH_3COO^-, and Cl^- ions on the morphology of calcium hydroxyapatite crystals. *Doklady Phys. Chem.*, 2007, **412**(1), 11–14 [translated from Russian].
31. Knoche, Eds. O., Kubaschewcki, O. and Hesselman, K., *Thermochemical Properties of Inorganic Substances, vol. 2*. Spinger-Verlag, 1991.
32. Cox, J. D., Wagman, D. D. and Medvedev, CODAT. A., *Key Values for Thermodynamics*. Hemisphere Publishing Corporation, NY, Washington/Philadelphia, L, 1989.
33. Orlovskii, V. P., Ionov, S. P., Belyaevskaya, T. V. and Barinov, S. M., Structural-thermodynamic model for synergisitic exchange of hydroxyl and fluoride ions in apatites with the participation of the carbonate ion. *Inorg. Mater.*, 2002, **38**(2), 182–184 [translated from Russian].